JOURNAL OF MATERIALS SCIENCE 25 (1990) 1237–1245

Phase stability and oxygen transport characteristics of yttria- and niobia-stabilized bismuth oxide

ASHOK V. JOSHI, SUDHIR KULKARNI, JESSIE NACHLAS, JORDAN DIAMOND, NEILL WEBER
Ceramatec, Inc., 2425 South 900 West, Salt Lake City, Utah 84119

ANIL V. VIRKAR
Department of Materials Science & Engineering, University of Utah, Salt Lake City, Utah 84112

As a part of an overall study to explore the potential application of stabilized Bi_2O_3 as oxygen separator in various electrochemical systems, an investigation of the stability and transport characteristics of yttria- and niobia-stabilized bismuth oxide was undertaken. Polycrystalline Bi_2O_3 samples containing 25 mol% Y_2O_3 were fabricated by pressureless sintering powder compacts at 1000° C in air. Samples containing 15 mol% Nb_2O_5 were also fabricated by pressureless sintering at 900° C in air. The resulting samples were dense and of an equiaxed microstructure with grain size in the range from 28 μm for the yttria-stabilized and 42 μm for the niobia-stabilized materials, respectively. X-ray diffraction of the as-sintered specimens showed them to be single phase with CaF_2-type structure. Ionic conductivity was measured by an a.c. technique over a wide range of temperatures. It was observed that the ionic conductivity of the yttria-stabilized bismuth oxide was greater than that of the niobia-stabilized one.

The specimens subsequently were annealed over a range of temperatures between 600° C and 700° C for up to several days. X-ray diffraction traces taken on the Y_2O_3-stabilized samples indicated that the original cubic solid solution had decomposed. The decomposition of the yttria-stabilized samples was also accompanied by the occurrence of exaggerated grain growth. The observed decomposition is not in agreement with the phase diagram available in the literature, according to which the cubic phase should be stable over the range of temperatures the samples were annealed in the present study. By contrast, Nb_2O_5-stabilized Bi_2O_3 remained cubic, although it appeared to have dissociated into two cubic solid solutions of slightly differing lattice parameters. There was no perceptible change in the grain size of the niobia-stabilized samples.

Several electrolyte tubes made of the yttria- and niobia-stabilized bismuth oxide were electrolytically tested under a d.c. mode with silver electrodes. In tubes made of the yttria-stabilized material, the current density decreased with time (under a constant applied voltage) at 650° C and at $\leqslant$ 700° C but did not at $\geqslant$ 700° C consistent with the observation that the material did not decompose at $\geqslant$ 700° C but did at 650° C. At 600° C, the rate of decrease was slower than at 650° C indicating that the kinetics of phase decomposition is probably slower at 600° C. In the niobia-stabilized tubes the decrease in the current density was lower. This decrease is probably related to the apparent formation of two cubic solid solutions of slightly differing compositions.

The present work shows that the published phase diagram of the Y_2O_3–Bi_2O_3 system is incorrect. The present results also suggest that for application to temperatures as low as 650° C (and possibly lower), electrolytes made with Nb_2O_5 as the stabilizer are preferable.

1. Introduction

The high temperature polymorph of Bi_2O_3 (often referred to as the δ-phase) is known to crystallize in the fluorite type of structure. The δ-phase is a defect fluorite with a large concentration of vacant sites on the oxygen sublattice [1, 2]. Stoichiometric δ-phase of Bi_2O_3 for example has 25% of the anion sites vacant. Under atmospheric conditions, Bi_2O_3 is an excellent oxygen ion conductor with very little electronic conduction when present as the δ-phase which is stable

0022–2461/90 $03.00 + .12

between 730° C and its melting point of 825° C [3–5]. The conductivity is orders of magnitude lower in the low temperature monoclinic phase. Also, in the monoclinic phase the conductivity is predominantly electronic [6, 7]. The narrow temperature range over which the δ-phase is stable implies that any practical utilization of this material is restricted to this range. Further, the transformation of the δ-phase to the monoclinic phase is accompanied by a large volume change which leads to the disintegration of the sample.

The work of Takahashi *et al.* [8, 9], however, has shown that the δ-phase can be retained to considerably lower temperatures by adding either Y_2O_3 or Gd_2O_3 as stabilizers. Work of Levin and Roth [10] shows that the cubic δ-phase can be stabilized to somewhat lower temperatures by the addition of various rare earth oxides. The cubic phase can also be stabilized by the addition of Nb_2O_5 [11] in which the cubic phase is stable down to ~610° C. Takahashi *et al.* [12] made several polycrystalline samples of Bi_2O_3–Nb_2O_5 of various compositions and determined their transport characteristics. The conductivity of samples containing 15 mol % Nb_2O_5, the composition which exhibited the highest conductivity, was $1.1 \times 10^{-2}\Omega^{-1}cm^{-1}$ at 500° C and $1.9 \times 10^{-1}\Omega^{-1}cm^{-1}$ at 700° C, respectively. Similarly, high ionic conductivities in Bi_2O_3 stabilized by the additions of Y_2O_3 and Gd_2O_3 have been documented by Takahashi and Iwahara [13] at temperatures as low as 500° C. These results would suggest that the Bi_2O_3–Y_2O_3 and Bi_2O_3–Gd_2O_3 solid solutions are stable at 500° C and thus may be potential candidates as electrolytes in electrochemical devices which depend upon the oxygen ion conduction characteristics of these materials.

The work by Datta and Meehan [14], who determined the Bi_2O_3–Y_2O_3 phase diagram, suggests that the cubic δ-phase can be stabilized down to ~500° C or even lower by the addition of over 25 mol % Y_2O_3. These authors, who used very high purity raw materials (greater than 99.99 %) to formulate samples of various compositions, reported considerable difficulty in attaining equilibrium. The significance of this will be discussed later.

The present work was motivated by the prospects of using stabilized bismuth oxide as an electrolyte in devices such as the oxygen pump and the oxygen heat engine. High ionic conductivity of stabilized bismuth oxide in comparison to zirconia makes it an ideal candidate as an electrolyte in applications involving moderately high partial pressures of oxygen such that thermodynamic stability of the electrolyte can be assured. (At 700° C, the decomposition potential of Bi_2O_3 is ~0.5 volt). Oxygen pump and oxygen heat engine are two such potential applications. It is imperative, however, that the electrolyte be stable for a period of time that exceeds the life expectancy of the device. The objective of the present work was to examine the stability of Y_2O_3–Bi_2O_3 and Nb_2O_5–Bi_2O_3 cubic solid solutions in air. Towards this end, dense samples in the form of pellets and tubes were fabricated by pressureless sintering of powder compacts in air. The samples were subsequently annealed for up to several days in air over a range of temperatures between 600° C and ⩾ 700° C. The samples were then examined by X-ray diffraction, scanning electron microscopy and optical microscopy. Electrical conductivity was measured by an a.c. technique. The time dependence of the conduction characteristics at a given temperature were determined by applying a fixed d.c. voltage across electrolyte tubes upon which silver electrodes were applied. After operating the cells in a d.c. mode for several hours to days, the electrolyte tubes were removed for further characterization which included X-ray diffraction analysis and an examination of the microstructure.

TABLE I Chemical analyses of the as-received powders.

Material	Assay	Impurities	Particle Size (μm)	Surface Area $(m\,g)^{-2}$
Bi_2O_3	99.9%	Al_2O_3–0.006% Sb_2O_3–0.005% SiO_2–0.006%	7.8	
Y_2O_3	99.99%	< 100 ppm	1.45	8.6
Nb_2O_5	99.5%	Ta–330 ppm Fe–300 ppm Si–300 ppm Al–100 ppm W–100 ppm Mg–50 ppm	– 325 mesh	

2. Experimental procedure

2.1. Fabrication of samples

Bi_2O_3*, Y_2O_3† and Nb_2O_5‡ ceramic powders were purchased from commercial vendors. Chemical analyses of the as-received powders supplied by the vendors are given in Table I. Conventional ceramic processing method was used for the fabrication of dense electrolytes which were formed in the form of pellets as well as one end closed tubes. For the fabrication of yttria-stabilized electrolytes, Bi_2O_3 and Y_2O_3 were weighed in desired proportions (25 mol % Y_2O_3, 75 mol % Bi_2O_3), mixed and ball milled for 12 h. After the milling process, PVB was added as a binder and again the powder mixture was milled for a half hour. The resultant mixture was dried at 80° C for 12 h in order to remove the organic liquids. The powder was then sieved through an 80 mesh screen. Pellets were green formed by die-pressing. Electrolyte tubes were green formed by isostatic pressing in a rubber mould with a stainless steel mandrel. Subsequently, the pellets and the tubes were sintered in air at 1000° C for 12 h. An essentially identical procedure was used for the fabrication of electrolytes of composition 15 mol % Nb_2O_5–85 mol % Bi_2O_3 except that these electrolytes were sintered at 900° C for 12 h.

2.2. Measurement of electrical conductivity

Electrical conductivity was measured by a.c.

*Ferro Corporation, Transelco Division, Penn Yan, N.Y. 14527.
†Molycorp, Inc., Unocal Company.
‡AESAR Group, Johnson Matthey, Inc., Seabrook, N.H. 03874.

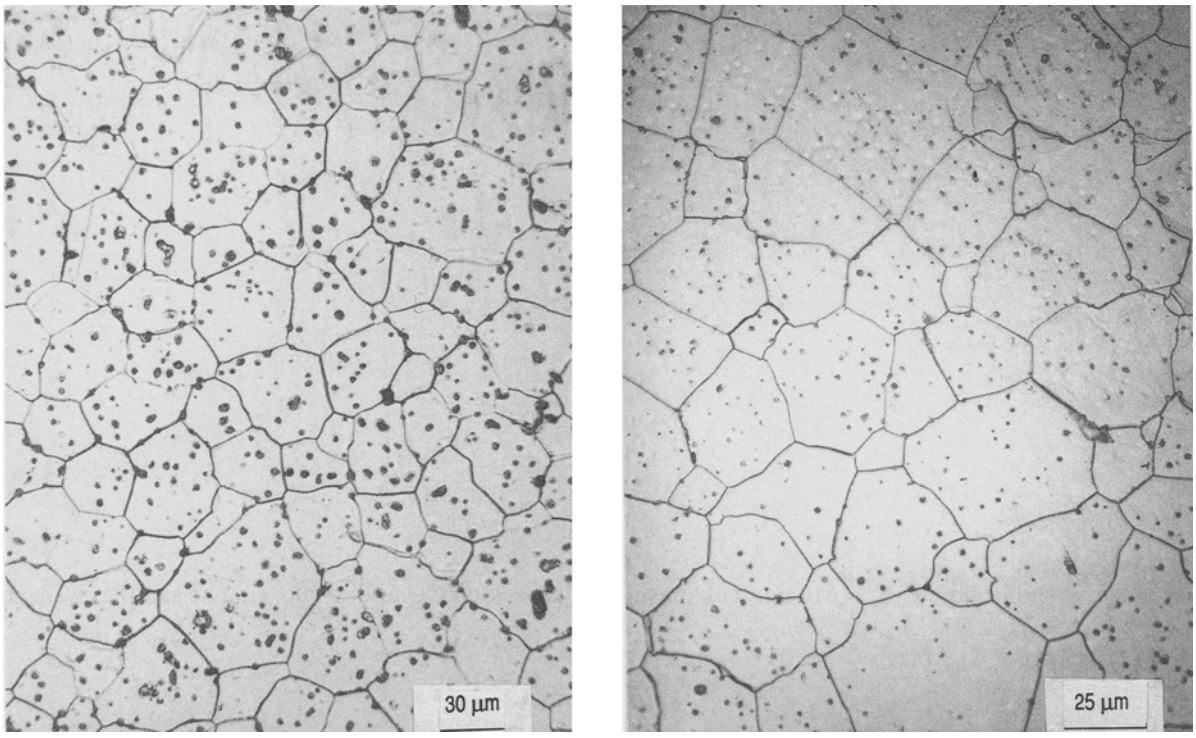

Figure 1 (a) An optical micrograph of an as-sintered sample containing 25 mol % Y_2O_3–75 mol % Bi_2O_3. The sample was sintered at 1000° C for 12 h. The polished sample was thermally etched at 975° C for 1 h to reveal the microstructure. The grain size is 28 μm; (b) An optical micrograph of an as-sintered sample containing 15 mol % Nb_2O_5–85 mol % Bi_2O_3. The sample was sintered at 900° C for 12 h. The polished sample was thermally etched at 850° C for 1 h to reveal the microstructure. The grain size is 42 μm.

technique using EG&G Impedance Bridge (System 368) with silver electrodes at a frequency of 1 kHz. The conductivity was measured in air over a range of temperatures between 600 and 800° C.

2.3. Electrolytic testing

Both the inside and the outside of electrolyte tubes were silver painted and silver wire leads were attached. The electrolyte tubes were then heated in air to 650° C in order that a good bond develops between the electrolyte and the silver electrodes. The tubes were then heated in tubular vertical furnaces and a small (0.2 volt) d.c. voltage was applied across the two silver electrodes. Electrolytic testing was done over a range of temperatures between 600° C and 800° C. For the determination of electrolyte stability, the tubes were maintained at 600° C, 650° C and $\geqslant$ 700° C for long periods of time while current was continuously passed through them. The tests were run under a constant total voltage and the total current was periodically measured. Some of the electrolyte tube segments were also annealed at various temperatures for up to several days under static conditions (without the passage of any current).

2.4. X-Ray diffraction and microscopy

X-ray diffraction patterns with CuKα radiation were obtained from the as-sintered and annealed samples as well as from those subjected to electrolytic testing. The tubes subjected to electrolytic testing were sectioned along the length of the tubes and patterns were obtained from each of the sections. X-ray diffraction traces were also obtained from samples that were subjected to annealing treatment without the passage of current. Samples were examined under a scanning electron microscope and an optical microscope in order to determine the microstructure of the as-sintered and the annealed samples.

3. Results and discussion

The densities of the as-sintered yttria- and niobia-stabilized bismuth oxide samples were 7.9 and 8.1 g ml^{-1}, respectively. Water immersion method indicated that the samples had sintered to the stage of closed porosity. Scanning electron and optical microscopy indicated that grain structures of the yttria- and niobia-stabilized samples were equiaxed with grain sizes on the order of 28 μm in the yttria-stabilized material and 42 μm in the niobia-stabilized material, respectively. The samples were thermally etched (Nb_2O_5–Bi_2O_3 at 850° C for 1 h and Y_2O_3–Bi_2O_3 at 975° C for 1 h) in order to reveal the grain boundaries. Figures 1a, and b show optical micrographs of the as-sintered samples of yttria- and niobia-stabilized bismuth oxide, respectively. X-ray diffraction traces of the as-sintered samples with either of the stabilizers showed the formation of a single cubic phase.

TABLE II Conductivity of yttria- and niobia-stabilized bismuth oxide

Composition	Temperature (K)	Conductivity (Ω^{-1} cm^{-1})
Bi_2O_3 + 25 mol % Y_2O_3	873	0.09
	973	0.18
	1073	0.31
Bi_2O_3 + 15 mol % Nb_2O_5	873	0.017
	973	0.04
	1073	0.06

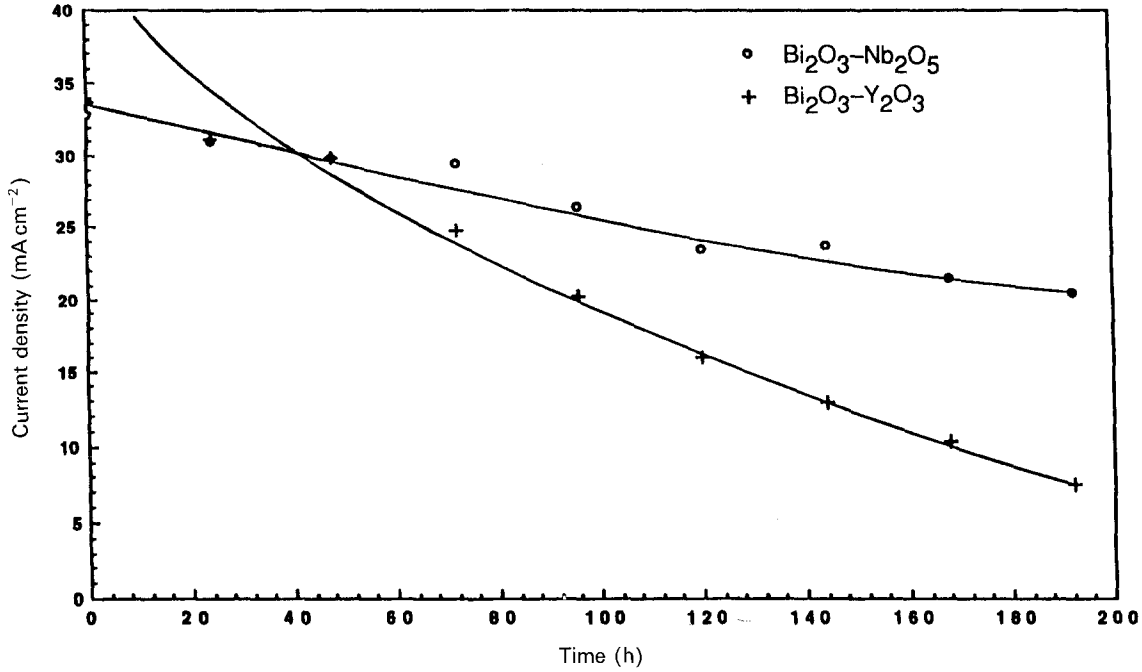

Figure 2 Current density as a function of time elapsed in yttria-stabilized and niobia-stabilized electrolytes at ~ 700° C under an applied voltage of 0.2 v.

Electrical conductivities measured in a d.c. mode for both yttria- and niobia-stabilized samples are given in Table II. As seen in the table, the conductivity of the yttria-stabilized bismuth oxide is consistently higher than that of the niobia-stabilized samples. This, of course, is to be expected because the incorporation of Nb_2O_5 in the lattice of Bi_2O_3 is expected to occur in such a way as to lower the concentration of oxygen vacancies as shown by the following defect reaction:

$$Nb_2O_5 + 2V_O^{\cdot\cdot} \rightarrow 2Nb_{Bi}^{\cdot\cdot\cdot} + 5O_O^x$$

The data in Table II show that the conductivity of Y_2O_3-stabilized Bi_2O_3 is about five times greater than that of Nb_2O_5-stabilized Bi_2O_3. This is partially reflected in the electrolysis experiments in that the extrapolated current density at zero time through the niobia-stabilized tubes was somewhat smaller than that through the yttria-stabilized tubes under the same applied voltage (actually the same electric field since the wall thicknesses of the two types of electrolyte tubes were identical). Figure 2 shows the current density as a function of time at approximately 700° C for both yttria- and niobia-stabilized tubes. The initial current density in both the yttria-stabilized and niobia-stabilized tubes was about 34 mA cm^{-2} although that extrapolated to zero time is about 40 mA cm^{-2}. This shows that the difference in the overall cell resistances in the yttria- and niobia-stabilized tubes is much smaller than expected on the basis of their conductivities indicating that most of the resistive losses occur at the electrode/electrolyte interfaces and/or within the electrodes themselves in the form of high sheet resistance. For example, under an applied voltage of 0.2 volt, the initial (extrapolated) current density was 40 mA cm^{-2} in the yttria-stabilized tubes. Wall thickness of the electrolyte tubes was 1 mm. Thus, of the 0.2 volt, 0.0222 volt corresponds to resistive loss in the electrolyte tube while the remaining 0.1778 volt must correspond to losses within the electrode, and/or at the electrode/electrolyte interfaces. These results suggest that the electrolyte resistance was not the dominating factor limiting current density in the present experiments. Under a d.c. mode, however, the current density in both of the cells (ytrria- and niobia-stabilized) continually decreased, with the decrease being considerably greater in the case of yttria-stabilized tubes. For example, after 190 h of operation, the current density in the yttria-stabilized tubes had decreased to under 10 mA cm^{-2}. By contrast, the current density in the niobia-stabilized tubes had dropped from 34 mA cm^{-2} to about 22 mA cm^{-2}. When both types of tubes were removed from the furnace, it was observed that silver electrodes had degraded to some extent. It appeared that the electrodes had become somewhat thinner. Since the vapor pressure of silver at ~ 700° C is significant, the loss of silver by evaporation is possible. However, the drastic decrease in current density in the yttria-stabilized

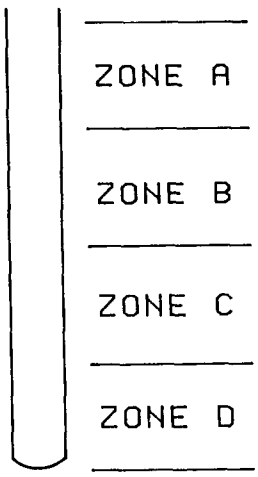

Figure 3 A schematic diagram showing the various sections of a yttria-stabilized electrolyte tube that was electrolytically tested with a temperature gradient *A* and *D*.

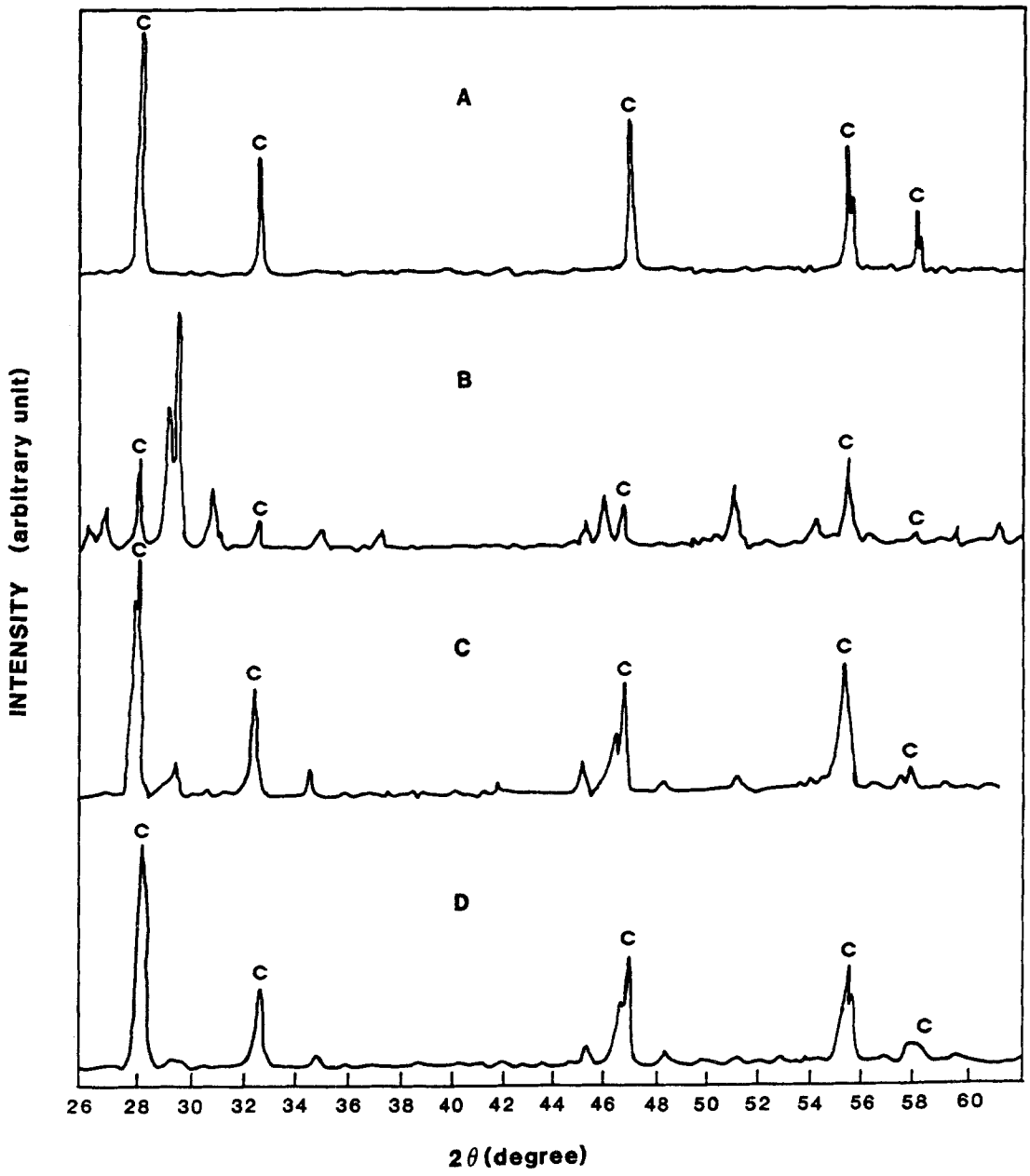

Figure 4 X-ray diffraction traces from the tube sections of the yttria-stabilized tube subjected to electrolytic testing under a temperature gradient: (*A*) The coldest end ($T_A \leqslant 500°$ C) showing a single phase cubic solid solution. (*B*) The cubic phase has partially decomposed and is now a minor phase. ($600°$ C $\leqslant T_B \leqslant 700°$ C) (*C*) Cubic phase is the majority phase although a substantial decomposition has occurred. ($600°$ C $\leqslant T_B \leqslant T_C \leqslant 700°$ C). (*D*) The hottest end. The majority phase is the cubic one with only a trace of the decomposed phase. ($T_D \approx 700°$ C).

tubes must be related to factors in addition to the degradation of the electrodes.

Interestingly, there were times when the current density in yttria-stabilized tubes at $\sim 700°$ C did not dramatically decrease. As mentioned earlier, the temperature in the furnace was approximately $700°$ C, often varying by as much as $\pm 15°$ C. The variability in the electrolytic behaviour was assumed to be related to temperature differences. In order to investigate the possible role of temperature, a cell was operated with a temperature gradient along the length of the tube. In this particular cell, the electrodes were applied along the length of the entire tube. The closed end of the tube was maintained at $\sim 700 \pm 5°$ C while the open end of the tube was under about $200°$ C. A d.c. current was passed through the tube for 200 h. Subsequently, the tube was cut into four sections *A*, *B*, *C*, and *D* as shown in Fig. 3 with *D* being from the hottest end and the *A* being from the coldest. The electrolyte tube segments were then examined by X-ray diffraction and microscopy. Figure 4 shows X-ray diffraction traces from each of the four sections. As seen in the figure, the trace of section *A* corresponds to the cubic, CaF_2-type structure and no other peaks are detected. The trace of segment *B* shows several other peaks in addition to the cubic peaks which are quite weak. Segment *C* shows the same peaks as segment *B* except that the cubic peaks are stronger while those of the other phase are weaker. Finally, segment *D*, which was in the hottest part of the furnace, shows nearly single phase cubic phase although a minor amount of the second phase is clearly evident in the pattern.

In the preceding experiments, the tubes were electrolytically tested. In order to ensure that the observed decomposition is temperature-related, a sample of the same composition was annealed at $650°$ C for 200 h

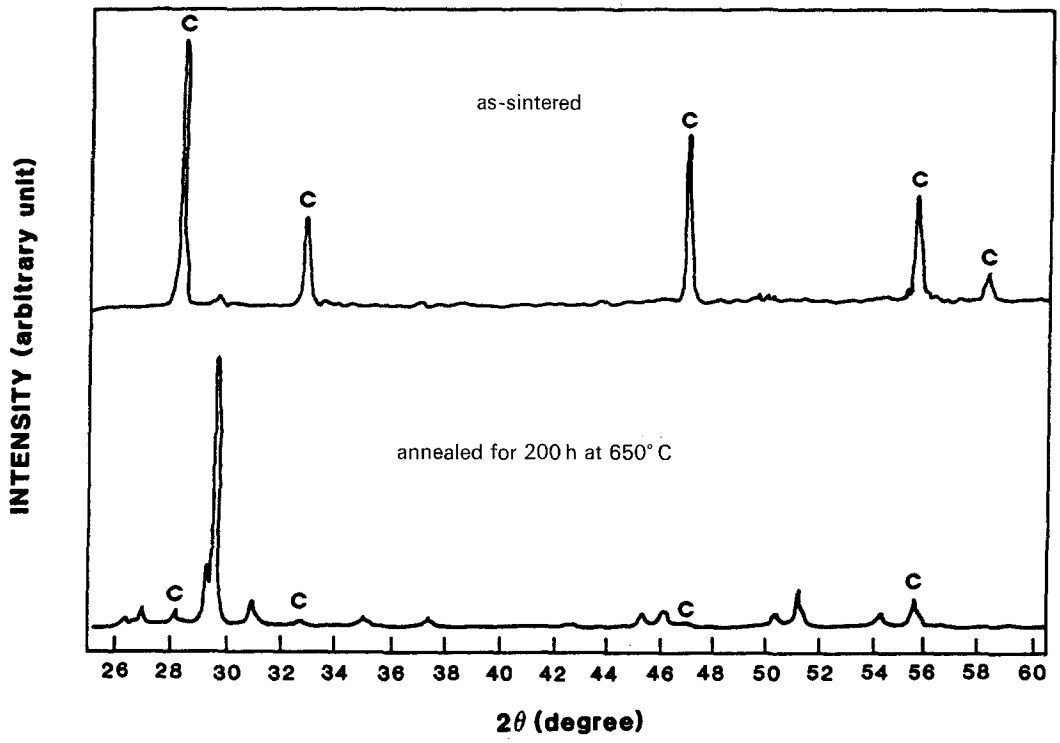

Figure 5 The effect of annealing at 650° C on the phase stability in Y_2O_3–Bi_2O_3 solid solutions: The as-sintered solid solution is cubic while only a trace of the cubic phase remains after annealing for 200 h at 650° C.

without the passage of current. As shown in Fig. 5, the cubic phase completely decomposed in 200 h at 650° C.

The fact that other peaks have appeared clearly indicates that the cubic phase in the Bi_2O_3–Y_2O_3 system is not stable under certain conditions. The temperature in the segment *B*, which showed the largest amount of the second phase(s), was less than 700° C but greater than about 600° C. The fact that trace amounts of the second phase(s) was detected in segment *D* suggests that the cubic phase is not stable at ~ 700° C. Presumably, the transition temperature, which was not determined in the present study, is slightly above 700° C. The reason that segment *B* has a considerably greater amount of the second phase(s) is that the kinetics of phase transformation must be more rapid at that temperature. In segment *C*, which was at a higher temperature, the amount of the second phase(s) was lower than in *B*. In segment *D*, which was at an even higher temperature, the amount of the second phase was smaller. These results indicate that phase transformation in this system probably occurs by conventional processes, such as nucleation and growth or cellular precipitation, kinetics of which depend upon two factors: mass transport processes, and thermodynamic driving force. The kinetics of phase transformation is expected to be describable by TTT (time–temperature–transformation) diagrams. The knee of the TTT curve probably is close to the temperature corresponding to the segment *B*. Slower kinetics at higher temperatures must be due to low driving force (thermodynamic limitation). Slower kinetics at lower temperatures (segment *A*), must be due to the kinetic limitation which in the present case is expected to be diffusional. That is, the kinetics are expected to be diffusion-limited at low temperatures.

The present results indicate that the cubic phase in the Bi_2O_3–Y_2O_3 system is unstable below about 700° C. The phase diagram given by Datta and Meehan [14], therefore, is incorrect. The possible reasons for this will be discussed later. The time dependence of the conduction characteristics follows a similar trend. Figure 6 shows the time dependence of the measured current density under a fixed applied potential at three temperatures, 700° C, 650° C and 600° C. As shown in the figure, the current density is nearly constant at 700° C for the duration of the experiment (~ 260 h). At 600° C the current density dropped to about 60% of the initial value. At 650° C, the current density dropped to 50% of the initial value indicating that the kinetics of decomposition are faster at 650° C than at 600° C and 700° C. These results suggest that the knee of the TTT curve is close to ~ 650° C. It is also conceivable that the degradation of the electrodes is less at 600° C.

As mentioned earlier, annealing experiments were also conducted under static conditions, i.e. under conditions when no current was passed through the electrolyte. The objective was to determine if the lack of stability of the cubic phase is somehow related to the electrolytic testing conditions. A sample containing 25 mol % Y_2O_3 was annealed at 650° C in air for 200 h. X-ray diffraction clearly showed the formation of second phase(s) suggesting that the instability of the cubic phase (δ-phase) is temperature-related.

Samples containing 15 mol % Nb_2O_5 as a stabilizer did not show formation of other phases even after annealing at 650° C for 200 h. However, some peak splitting of the cubic peaks was observed. Typical diffraction traces of the as-sintered and annealed samples are shown in Fig. 7a and b, respectively. The

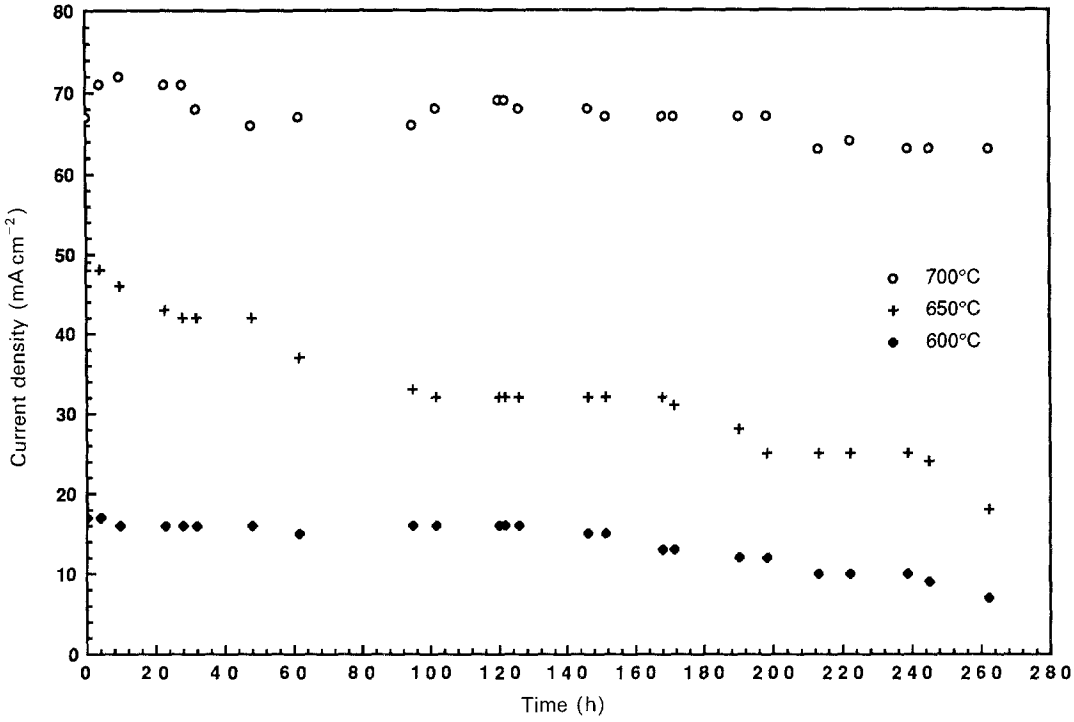

Figure 6 The dependence of the current density under a fixed applied d.c. potential (0.2 v) in yttria-stabilized bismuth oxide tubes at 600° C, 650° C and 700° C.

splitting of the peaks suggests the formation of two cubic phases (of CaF2 structure) of slightly different compositions. Lattice parameters of the two phases were determined to be 5.49 nm and 5.51 nm, respectively. The observed peak splitting increased with increasing 2θ angle. The pattern seems to indicate the presence of two cubic solid solutions of differing compositions.

In the Y_2O_3–Bi_2O_3 system, it was observed that phase transformation is accompanied by a substantial grain growth. Figures 8a and b show scanning electron micrographs respectively of the as-sintered and annealed (at 650° C for 200 h) samples containing 25 mol % Y_2O_3. The microstructure of the as-sintered sample is relatively fine grained. However, the annealed sample exhibits the presence of very large grains. The annealed samples were also very fragile. By contrast, as shown in Figs 9a and b, no noticeable change occurred in samples containing 15 mol % Nb_2O_5 even after annealing at 650° C for 200 h. Similarly, Y_2O_3–Bi_2O_3 samples annealed above 700° C do not exhibit exaggerated grain growth. This suggests that the

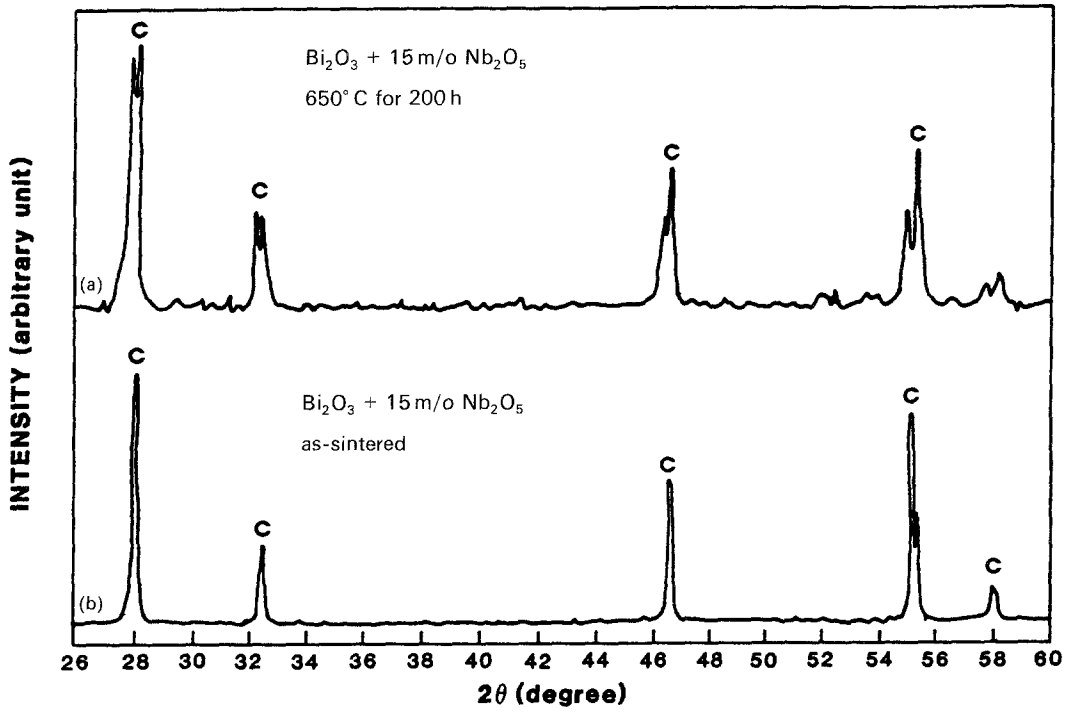

Figure 7 (a) X-ray diffraction trace of the as-sintered 15 mol % Nb_2O_5–85 mol % Bi_2O_3 ceramic showing a single phase cubic solid solution; (b) X-ray diffraction trace of the niobia-stabilized tube after annealing at 650° C for 200 h in air. As seen in the figure, the cubic peaks exhibit peak splitting indicating the formation of two cubic solid solutions.

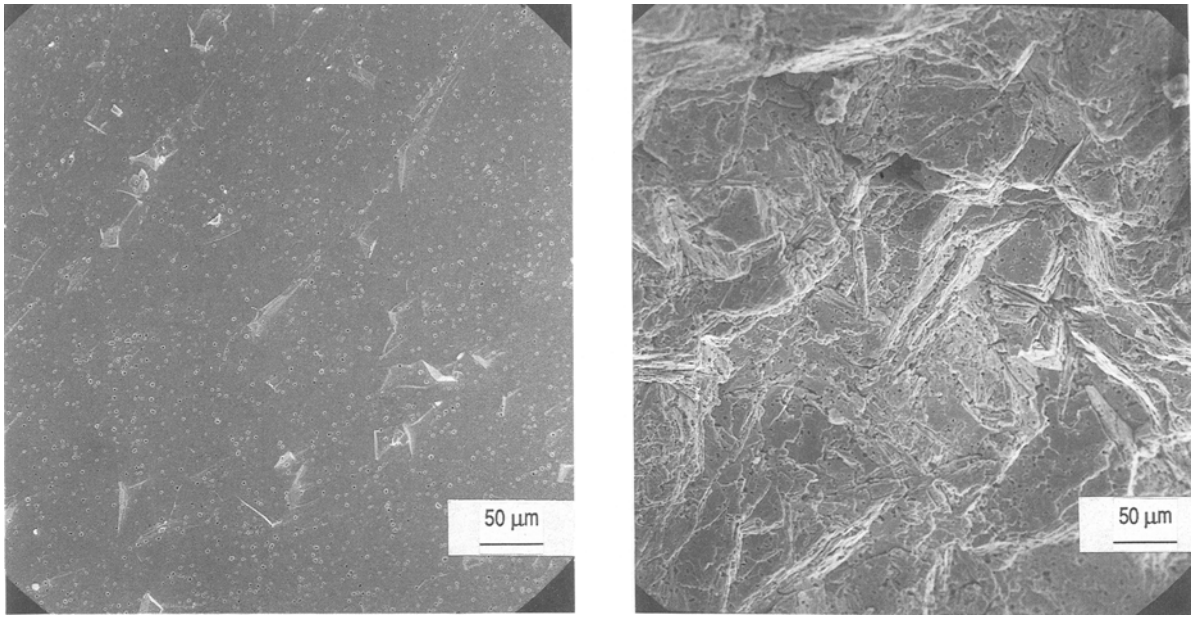

Figure 8 (a) A scanning electron fractograph of an as-sintered Y_2O_3–Bi_2O_3 ceramic.; (b) A scanning electron micrograph of a Y_2O_3–Bi_2O_3 ceramic that had been annealed for 200 h at 650° C showing the presence of large grains.

occurrence of exaggerated grain growth is related to the phase transformation.

For the determination of the Y_2O_3–Bi_2O_3 phase diagram, Datta and Meehan [14] used very high purity materials; purities greater than 99.99%. Considerable difficulties were experienced in achieving equilibrium. As discussed in the following, the use of ultra high purity materials may be the principal factor which prevented the establishment of equilibrium conditions in the work of Datta and Meehan [14]. At any given temperature, the formation of the equilibrium phases of equilibrium compositions starting from an initial single phase solid solution requires that the samples are annealed for long enough time for mass transport processes driven by chemical free energy changes are complete, or nearly complete. Mass transport in these materials is expected to occur via point defects. Since both bismuth and yttrium are trivalent, no additional, valence-related point defects are created by the incorporation of Y_2O_3 in Bi_2O_3. If the two oxides are very pure, so will be the solid solution. This would mean very low concentrations of point defects would be available for mass transport processes to occur. The solid solution is then near "intrinsic" conditions, i.e., the cation vacancy concentration would be about the same as the cation interstitial concentration and would be given by the square root of the pertinent Frenkel product. (The preceding assumes that the solid solution is stoichiometric under atmospheric oxygen partial pressure.) For example, if the Frenkel product of the solid solution on the cation sublattice is K_F, the vacancy and interstitial concentrations are

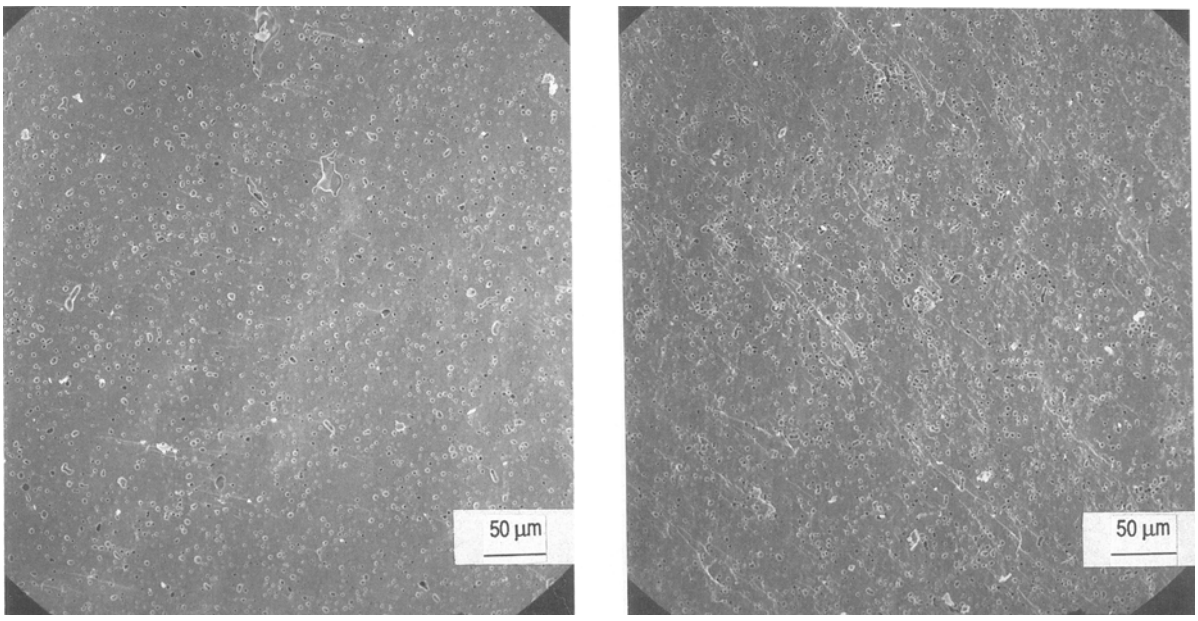

Figure 9 (a) A scanning electron micrograph of an as-sintered Nb_2O_5–Bi_2O_5 ceramic; (b) A scanning electron micrograph of a Nb_2O_5–Bi_2O_3 sample that had been annealed at 650° C for 200 h. As seen in the micrograph no change in the grain size occurred.

given by

$$[V^{\cdots}_{Bi,Y}] = [I^{\cdots}_{Bi,Y}] = \sqrt{K_F} \quad (1)$$

Under intrinsic conditions, the concentrations at low temperatures are expected to be very low. As a result, the interdiffusion coefficient, D, on the cation sublattice given by* [15]

$$D = \frac{D_{Bi}D_Y}{X_{Bi}D_{Bi} + X_YD_Y} \quad (2)$$

is very low if the intrinsic or near-intrinsic conditions prevail. In the above equation, D_{Bi} & D_Y and X_{Bi} & X_Y are diffusion coefficients and mole fractions of Bi and Y in the solid solution, respectively. For phase separation to occur, it is essential that Bi and Y ions diffuse on the cation sublattice. It is not necessary for the oxygen ions to move as oxygen is common to both of the oxides. The kinetics of phase transformation is enhanced if the interdiffusion coefficient on the cation sublattice is enhanced. Under near-intrinsic conditions, the interdiffusion coefficient is very low and therefore the kinetics of phase transformation are also slow. If aliovalent impurities are present, either the cation vacancy concentration or the cation interstitial concentration will be considerably greater than the intrinsic concentration $\sqrt{K_F}$.

For example, if the impurity is of a higher valence than the host cations (greater than 3) then $[V^{\cdots}_{Bi,Y} \gg \sqrt{K_F}$. Alternatively, if the impurity is of lower valence (less than 3), then $[I^{\cdots}_{Bi,Y}] \gg \sqrt{K_F}$.

It can be shown that the interdiffusion in such a case can be higher than that in the intrinsic conditions regardless of the valence of the dopant (i.e. either higher or lower than 3 but not 3) provided the concentration of the impurity is sufficiently large so as to offset the relative differences in the defect diffusivities. The effect of aliovalent impurities on the kinetics of phase transformation in two ceramic systems; namely TiO_2–SnO_2 and $LiAl_5O_8$–$LiFe_5O_8$, has been demonstrated recently by Virkar *et al.* [16–19]. The general conclusions of the work on phase transformation kinetics are that aliovalent impurities affect the kinetics of phase transformation significantly and that the use of ultra high purity materials for the determination of phase diagrams may be unadvisable in a large number of cases.

In the work of Datta and Meehan [14] who used very high purity materials, near-intrinsic conditions must have prevailed thereby rendering the kinetics of mass transport very sluggish. It thus appears that equilibrium conditions were not established in their work. As such the phase diagram given by these authors is not a true equilibrium phase diagram. This is evidenced by the fact that when annealed at $\sim 700°C$ or at lower temperatures, the cubic solid solution decomposes.

The present results suggest that for applications below about 700° C (and above 650° C), niobia-stabilized bismuth oxide is preferable to the yttria-stabilized material despite the higher ionic conductivity of the yttria-stabilized bismuth oxide. The present work also shows that the current density through niobia-stabilized tubes was about the same as that can be passed through yttria-stabilized tubes. This, however, is a drawback and not an advantage for it shows that the voltage drop across the electrode/electrolyte interface is too large compared to that through the electrolyte. For example, at 700° C, the voltage drop across the electrode/electrolyte interface was in the neighbourhood of 80 to 90%. This is simply too large for any device through which significant amounts of current must pass. Potential application of these materials in devices such as the oxygen heat engine or the oxygen pump must await the development of suitable electrodes.

Acknowledgements

This work was supported SDIO/IST and managed by the Office of Naval Research under Contract No. N00014-86-C-0827. Dr James Auburn of AT and T was the project monitor.

References

1. G. GATTOW and H. SCHRÖDER, *Z. Anorg. Allg. Chem.* **318** (1962) 176.
2. G. GATTOW and D. SCHULTZE, *Z. Anorg. Alleg. Chem.* **328** (1964) 44.
3. M. G. HAPASE and V. B. TARE, *Indian J. Pure Appl. Phys.* **5** (1967) 401.
4. T. TAKAHASHI, H. IWAHARA and Y. NAGAI, *J. Appl. Electrochem.* **2** (1972) 97.
5. T. TAKAHASHI and H. IWAHARA, *J. Appl. Electrochem.* **3** (1973) 65.
6. R. MANSFIELD, in Proceedings Physics Society, London **62** (1949) 476.
7. H. A. HARWIG and A. G. GERARDS, *J. Solid State Chem.* **26** (1978) 265–74.
8. T. TAKAHASHI, H. IWAHARA and T. ARAO, *J. Appl. Electrochem.* **5** (1975) 187.
9. T. TAKAHASHI, T. ESAKA and H. IWAHARA, *J. Appl. Electrochem.* **5** (1975) 197.
10. E. M. LEVIN and R. S. ROTH, *J. Res. Natl. Bur. Standards* **68A** [2] (1964) 200.
11. R. S. ROTH and J. WARING, *J. Res. Natl. Bur. Standards* **66A** [6] (1962) 461.
12. T. TAKAHASHI, H. IWAHARA and T. ESAKA, *J. Electrochem. Soc.* **124** [10] (1977) 1563.
13. T. TAKAHASHI and H. IWAHARA, *Mater. Res. Bull.* **13** (1978) 1447.
14. R. K. DATTA and J. P. MEEHAN, *Z. Anorg. Allg. Chem.* **383** [3] (1971) 328.
15. A. R. COOPER, JR and J. H. HEASLEY, *J. Amer. Ceram. Soc.* **49** [5] (1966) 280–4.
16. A. V. VIRKAR and M. R. PLICHTA, *J. Amer. Ceram. Soc.* **66** [6] (1983) 451–6.
17. T. C. YUAN and A. V. VIRKAR, *J. Amer. Ceram. Soc.* **71** [1] (1988) 12–22.
18. S. J. KIM, Z. C. CHEN and A. V. VIRKAR, *J. Amer. Ceram. Soc.* **71** [10] (1988) C428–C432.
19. R. M. COHEN, D. DROBECK and A. V. VIRKAR, *J. Amer. Ceram. Soc.* **71** [9] (1988) C401–C403.

Received 28 November 1988
and accepted 8 May 1989

*This assumes that the anions are immobile. In Y_2O_3–Bi_2O_3, however, oxygen is highly mobile. Thus this equation is not strictly valid. It may continue to be valid if the chemical potential of oxygen ions is uniform everywhere so that no driving force exists for its diffusion.